7. Terrestrial Acidification

Ligia B. Azevedo[1,2], Pierre-Olivier Roy[3], Francesca Verones[1], Rosalie van Zelm[1], Mark A. J. Huijbregts[1]*

[1] Radboud University Nijmegen, Department of Environmental Sciences, Toernooiveld 1, 6500 GL Nijmegen, the Netherlands

[2] International Institute for Applied Systems Analysis, Ecosystem Services and Management Program, Schlossplatz 1, A-2361 Laxenburg, Austria

[3] CIRAIG, Chemical Engineering Department, École Polytechnique de Montréal, P.O. Box 6079, Montréal, Québec, Canada, H3C 3A7

* azevedol@iiasa.ac.at

Based on: Roy *et al.* (2012b), Roy *et al*. (2012a), Roy et al. (2014), and Azevedo *et al.* (2013).

7.1.   Environmental mechanism and impact categories covered

Terrestrial acidification is characterized by changes in soil chemical properties following the deposition of nutrients (namely, nitrogen and sulfur) in acidifying forms. Here, we assess the environmental impact of nitrogen oxides (NO_x), ammonia (NH_3), and sulfur dioxide (SO_2), see Figure 7.1. In addition to soil pH decline (i.e. increase in hydrogen cation concentration in the soil), the increase in acidifying nutrients concentration in the soil leads to the decline in base saturation and the increase of aluminum dissolved in soil solution. This decline in soil fertility may lead to an increase in plant tissue yellowing and seed germination failure and a decrease in new root production, thereby reducing photosynthetic rates and plant biomass and, in extreme cases, plant diversity (Falkengren-Grerup 1986; Roem et al. 2000; Zvereva et al. 2008).

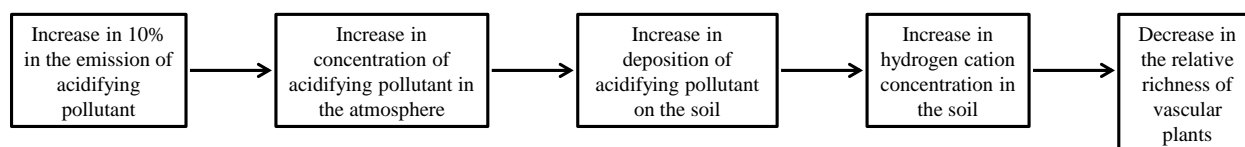| Increase in 10% in the emission of acidifying pollutant | → | Increase in concentration of acidifying pollutant in the atmosphere | → | Increase in deposition of acidifying pollutant on the soil | → | Increase in hydrogen cation concentration in the soil | → | Decrease in the relative richness of vascular plants |

Figure 7.1: Illustration of the impact pathway represented in equation 7.1.

The impact category covered by this environmental mechanism is the ecosystem quality. The acidification impact is related to the atmospheric transport of the emitted pollutants and their subsequent impact on soil pH (described by the fate factor), and to the sensitivity of the ecosystem to soil acidity (described by the effect factor). Here, the effect factor is based on the decline in richness of vascular plants. Note that in cases where acidifying pollutants are released to human-built structures (e.g. buildings and statues) there can be aesthetic impacts of terrestrial acidification. However, this mechanism is not taken into account in this framework.

The coverage of the endpoint characterization factor (CF) is global. Of the three effect factor models (i.e. linear, marginal, and average approaches), we chose the marginal one. The spatial resolution of the CF is 2.0° x 2.5°.

7.2. Calculation of the characterization factors at endpoint level

An endpoint characterization factor (yr·kg^{-1}, see Figure 7.1 for illustration of impact pathway) for emitting cell i for pollutant p (i.e. NO_x, NH_3, or SO_2) is described as

$$CF_{end,i,p} = \sum_{j,p} AF_{i \to j,p} \cdot SF_{j,p} \cdot EF_j$$

<div align="right">Equation 7.1</div>

where $AF_{i \to j,p}$ is the atmospheric fate factor of pollutant p from cell i to receiving cell j, $SF_{j,p}$ is the soil sensitivity factor, and EF_j is the effect factor in cell j.
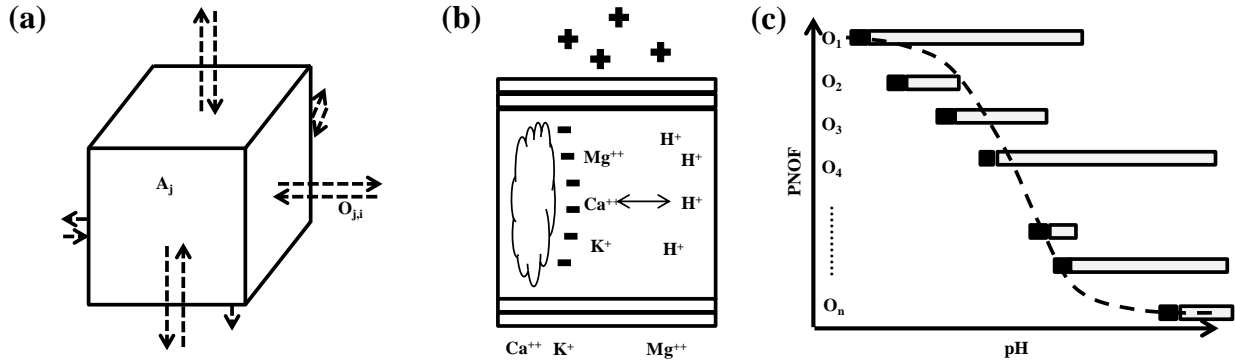

Figure 7.2: Illustration of the (a) atmospheric transport, adapted from Roy *et al.* (2012b), (b) soil chemistry, and (c) the logistic regression originating effect model, adapted from Azevedo (2014). In (a), the flows through six possible transport pathways into and out of a receiving cell j (one pathway represented by $O_{j,i}$) and the accumulated mass of pollutant in j (A_j) in the atmospheric compartment are used in a mass balance of the source-receptor matrix (SRM). In (b), the flow of positively charged ions (+) originating from the dissociation of sulfuric acid and nitrous acid and from the reduction of ammonia prompts base cations to be leached out of the soil profile (here, the middle soil layer is amplified for illustration purposes). In (c), the potentially not occurring fraction (PNOF) of species as a logistic function of pH is determined with the lowest tolerable pH condition (illustrated as the black tip of the grey bar pH range) for individual species (O_i) recorded in observational field studies.

<u>Atmospheric fate factor</u>

The atmospheric fate factor (keq·ha^{-1}·kg^{-1}) is described as

$$AF_{i \to j,p} = \frac{dDEP_{j,p}}{dEM_{i,p}}$$

<div align="right">Equation 7.2</div>

where dDEP (keq·yr^{-1}·ha^{-1}) is the relative increase in deposition of pollutant p onto the terrestrial compartment j following an increase in the emission of p from emitting cell i, dEM (kg^{-1}·yr), by 10% relative to a reference year (2005) (Roy et al. 2012b).

The unit of the AF is given as kiloequivalent of electric charge (keq) per mass of emitted pollutant per given area (therefore, keq·ha^{-1}·kg^{-1}). (The unit of electric charge can be converted from a mass of deposited pollutant by taking the atomic weight and the valence of the atom deposited. For example, 1 mol of sulfur is equal to 64.13eq, because the atomic weight of S is 32.07 and its valence is 2).

The AF is derived based on the tropospheric chemistry model GEOS-Chem, which is described in detail by Roy *et al.* (2012b). It considers various photochemical reactions and the flow of particles that is influenced by temperature and atmospheric pressure differences, described in detail by Evans & Jingqiu (2009). The model includes transboundary transport across countries and across continents. The inventory of emissions in 2005 includes anthropogenic sources, e.g. fossil fuel, and biofuel, and biomass burning as well as non-anthropogenic sources (for example, sulfur in volcanic ash and nitrous oxides from soils and produced with lightning). Note that the AF describes a relative change in emissions from a given year. Thereby the inclusion of natural sources of acidifying pollutants should not influence the estimation of the environmental impact as long as the reference year is

representative of other years. The year of 2005 is chosen since it is a representative average of the period from 1961 to 1990 according to the National Climatic Data Center of the National Oceanic and Atmospheric Administration (NOAA 2005).

The atmospheric fate model consists of a three-dimensional transport from emitting cell i to receptor cell j and is calculated with a source-receptor matrix (SRM) of the transport of pollutant p within the atmospheric compartment in six possible directions, i.e. latitude-wise (north and south), longitude-wise (east and west), and altitude-wise (upwards and downwards), with a total of 615,888 compartments included in the SRM. The SRM is the pollutant mass balance of the mass of emitting cells. The mass across all receiving compartments are equal for a given year (in this case, 2005), see illustration in Figure 7.2a.

Soil sensitivity factor

The soil sensitivity factor (mol H·L^{-1}·ha·keq^{-1}·yr) is described as

$$SF_{j,p} = \frac{dC_j}{dDEP_{j,p}}$$

Equation 7.3

where dC$_j$ is the increase in hydrogen ion concentration (mol H·L^{-1}) following an increase in dDEP for pollutant p in receiving cell j. The SF is derived based on the steady-state soil chemistry model PROFILE and is described in detail by Roy $et\ al.$ (2012a). It includes various parameters of soil chemistry (e.g. dissolved organic carbon, soil bulk density and texture) and climate (i.e. precipitation and temperature). The model consists of a two-dimensional mass balance of positive ions originating from atmospheric deposition. The exchanges of cations include soil chemical reactions with hydrogen ions, aluminum, base cations (i.e. potassium, calcium, and magnesium), and silicon.

The mass balance was performed in each receiving cell j, with resolution 2.0° x 2.5° worldwide (and, thus, 99, 515 cells in total), across five 20cm soil layers of the first meter of soil, see illustration in Figure 7.2b. The total impact on the five soil layers of cell j was weighted based on the fraction of roots in each layer. The distribution of roots in the first meter of soil was reported by Jackson $et\ al.$ (1996) for each of the fourteen terrestrial world biomes. We used the biome map provided by Olson $et\ al.$ (2001) to define the biome occupying each cell j. The parameters for the SF calculation are reported by Roy $et\ al.$ (2012a).

Effect factor

The effect factor (mol H^{-1}·L) is described as

$$EF_j = \frac{SD_j \cdot A_j \cdot MEF_j}{S_{global}}$$

Equation 7.4

where MEF is the marginal effect factor (mol H^{-1}·L), A$_j$ refers to the terrestrial ecosystem area in grid cell j (ha), SD$_j$ is the species density of vascular plant species in grid cell j (species/ha) and S$_{global}$ is the total number of plant species taken from Kier et al. (2009), which is 315'903.
Note that the unit of the EF is the loss of vascular plant species in j relative to the total number of vascular plant species worldwide per mol/l increase of H+ concentration. In this work, we equate potentially not occurring fraction with PDF. This relationship allows for an estimation of the actual potential global species loss.

The vascular plant richness density SD is derived from the vascular plant richness (see illustration in Figure 7.3), derived by Kier et al. (2009), and the area of each region.

The marginal effect factor is described as

$$MEF_j = \frac{dPDF_j}{dC_j} = \frac{dPNOF_j}{dC_j}$$ **Equation 7.5**

where dPDF and dPNOF are the marginal increase in the potentially disappearing and not occurring fractions (both dimensionless) following a marginal increase in dC_j in j. Since the EF describes a marginal increase to PDF, the reference state for the changes in PDF is the PNOF prior to the increase in hydrogen ion concentrations in the soil.

The EF model is based on a probabilistic model of the PNOF as a logistic function of hydrogen ions (Equation 7.6) and it is described in detail by Roy et al. (2014). The logistic function describes the cumulative fraction of absent species with increasing hydrogen ion concentration, Figure 7.2c. The inputs for the derivation of the EF are the two parameters of the logistic function, i.e. the ion concentration at which PNOF is 0.5 (α) and the slope of the function (β), and the hydrogen ion concentration resulting from the acidic deposition in receiving cell j, C_j.

$$PNOF_j = \frac{1}{1+e^{-\frac{log_{10}C_j - \alpha_j}{\beta_j}}}$$ **Equation 7.6**

The two logistic function parameters (α and β) were derived at resolution of biome and the hydrogen ion variable, C_j, was derived for each 2.0° x 2.5° receiving cell j with the PROFILE model. The biome-specific α and β parameters were derived from logistic regressions which used the maximum tolerance hydrogen ion concentration of each species subsisting in that biome, see illustration in Figure 2c. Species-specific data on minimum tolerable pH per biome (from which maximum hydrogen ion concentration in cell j, C_j, were derived) were reported by Azevedo *et al.* (2013). The biome-specific parameters for the EF calculation are shown in Figure 7.5. Grid-specific CFs are shown in Figure 7.4. Country, continent, and world CFs were derived based on a weighted average of emissions of SO_2, NH_3 and NO_x repsectively (IIASA 2015), within the aggregation unit level (see Excel file and Tables 7.1 and 7.2). Global average values are 5.2E-14 PDF·kg^{-1}·yr, 2.5E-14 PDF·kg^{-1}·yr and 1.0E-14 PDF·kg^{-1}·yr for SO_2, NO_x and NH_3, respectively.
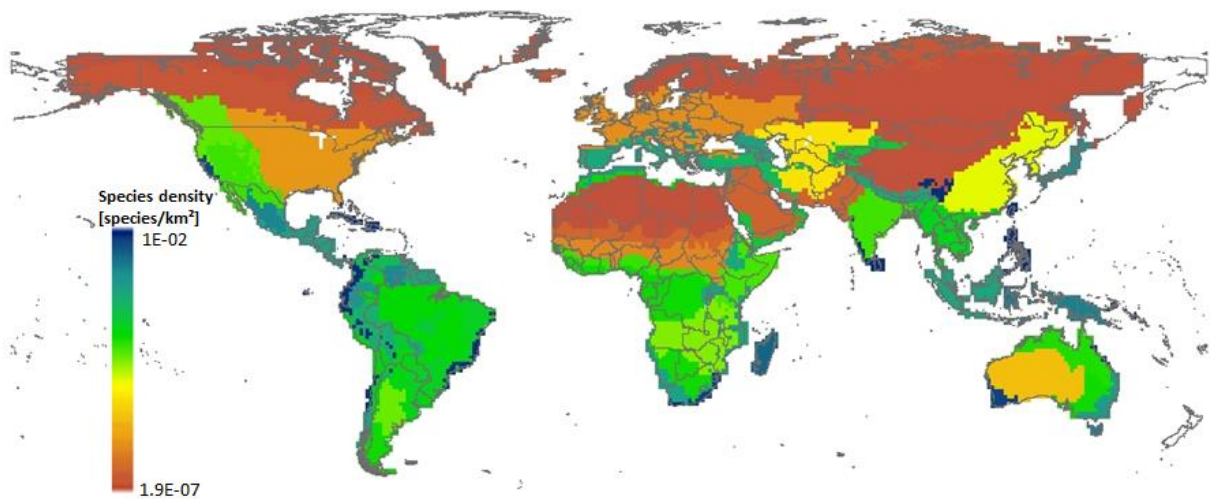

Figure 7.3: Relative species richness of vascular plants (species·km^{-2}) derived from Kier et al. (2009).

Soil chemical processes, estimated by Roy *et al.* (2012a), contribute the most to the variance in the NO_x, NH_3, and SO_2 emission impacts (Roy et al. 2014). The uncertainty in the parameters on which the EF is based contributes the most to the variability in the effect factors.

7.3.   Uncertainties

The fate factors for terrestrial acidification are based on an atmospheric deposition and on a chemical soil property model, whereby an increase in 10% of atmospheric emission of an acidifying pollutant prompts an increase in atmospheric deposition and, consequently, an increase in hydrogen ions in soil solution (Roy et al. 2012a; Roy et al. 2012b). The atmospheric model includes transport across continents and it depends upon the dispersion of the pollutant, weather characteristics, and the locations of emission and deposition. The soil sensitivity model is influenced by the capacity of the receiving soil to buffer acidifying pollutants and fraction land in the receiving grid.

The atmospheric fate and soil sensitivity models can also be verified by comparison with an existing endpoint characterization model covering Europe (van Zelm et al. 2007). This comparison is skewed since the transportation pathways of N and S forms are not exactly the same for both fate models. van Zelm *et al.* (2007) do not account for transboundary atmospheric transport beyond Europe as the model is limited to that continent. Additionally, the stressor indicating acidification is not the same (base saturation in the model by van Zelm *et al.* (2007) and pH in the model of (Roy et al. 2014).

There is sufficient evidence of the detrimental impact of terrestrial acidification on the performance of plants (Falkengren-Grerup 1986; Zvereva et al. 2008). Thus, the level of robustness of impact is fairly high. However, the effect model used to derive endpoint effect factors employs observational field data whereby the absence of species resulting from decreasing pH cannot be confirmed and, thus, proof of causality is problematic. Proof for causality would only be possible if the underlying data would consist of controlled (not observational) experiments in which the high level of a stressor (in this case, high hydrogen ion levels) would be the primary cause for a species becoming absent.

The failure to record the species at a specific pH may be human related, such as (1) an incomplete survey of the existing species or of the existing pH, but also due to natural causes, such as that (2) the species may be rare and difficult to spot, (3) extreme pH may be tolerated by the species but may not be found under natural conditions, or (4) the pH is tolerated by the species but the species absence is due to another stressor. For a detailed description of the downsides of observational field data for conducting impact assessments, see Azevedo (2014). Because of the possible underestimation of the minimum pH tolerated by the species, the level of evidence of the effect model specifically employed here is considered low.

The variance across CFs is most explained by either the atmospheric fate factor or the soil sensitivity factor, depending on the pollutant considered (Roy et al. 2014).

7.4.   Value Choices

The time horizon for this impact category is not relevant since it is assumed that the impact occurs at the moment of emission of NO_x, NH_3, or SO_2 to the atmospheric compartment. No choices are thus modelled for fate and effect factor for terrestrial acidification. In total, the CFs are considered as low level of robustness, mainly because one out of the two pollutants of acidification (i.e. N) is also included in terrestrial eutrophication. It is therefore not possible to disentangle if detrimental effects are due to the increase in hydrogen ions (acidification) or increase in primary productivity (eutrophication).
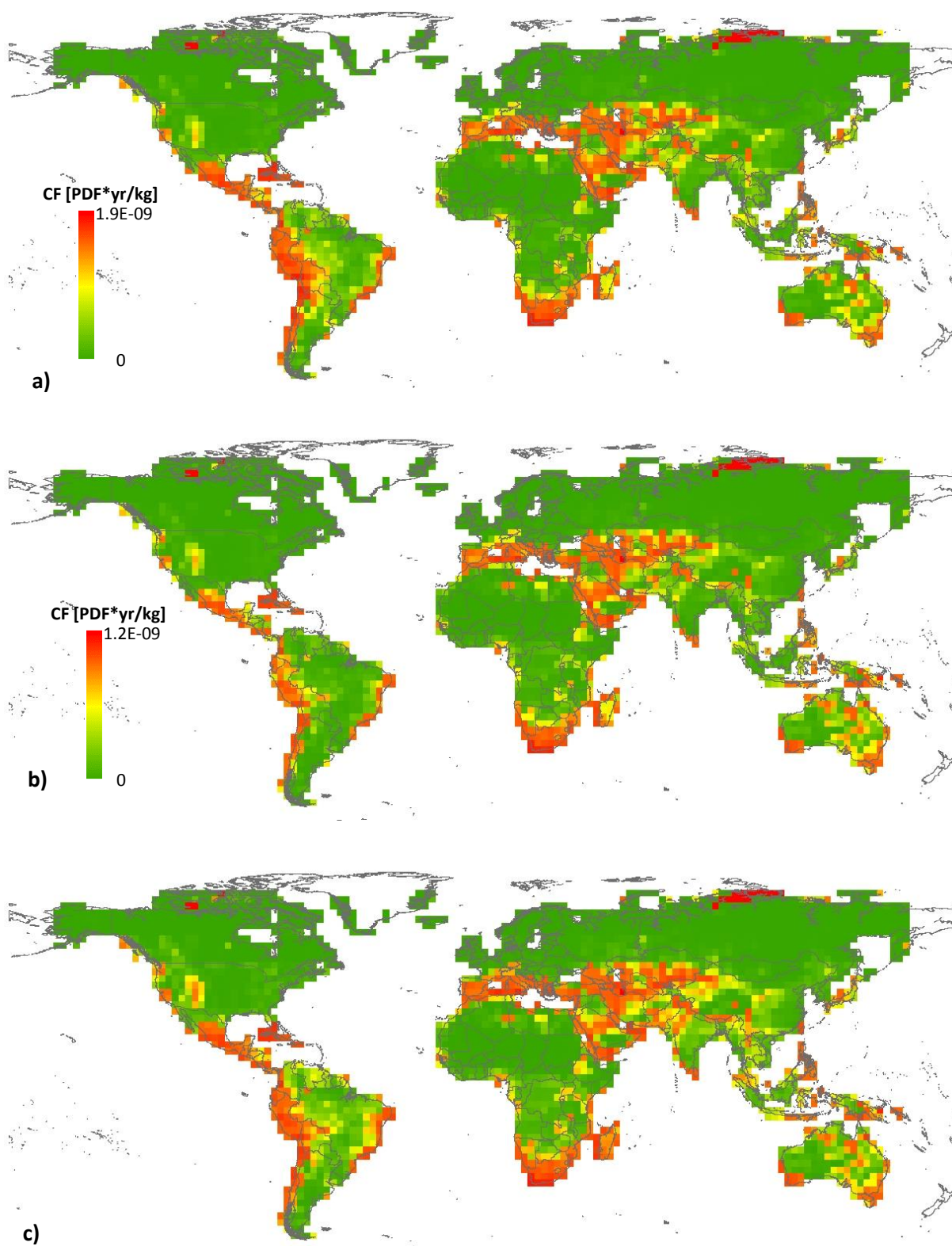
Figure 7.4: Endpoint characterization factors (PD·Fkg^{-1}·yr) based on vascular plant richness for (a) SO$_2$, (b) NO$_x$, and (c) NH$_3$.

Table 7.1: Global endpoint characterization factors (PD·Fkg⁻¹·yr) on a country level, based on vascular plant richness for SO₂, NOₓ, and NH₃. The relevant compartment here is the soil.

COUNTRY	CF SO$_2$ [PDF·yr/kg]	CF NOx [PDF·yr/kg]	CF NH$_3$ [PDF·yr/kg]
Afghanistan	8.49E-16	8.23E-16	1.70E-15
Albania	1.32E-13	5.95E-14	4.41E-14
Algeria	3.99E-15	4.10E-15	5.97E-15
Angola	5.88E-16	8.55E-16	5.54E-16
Antarctica			
Argentina	1.27E-15	1.11E-15	3.15E-16
Armenia	0.00E+00	0.00E+00	0.00E+00
Australia	2.12E-14	6.09E-14	8.41E-15
Austria	3.86E-15	1.28E-15	2.78E-15
Azerbaijan	2.58E-14	3.38E-14	4.72E-14
Azores	0.00E+00	0.00E+00	0.00E+00
Bahamas	0.00E+00	0.00E+00	0.00E+00
Bangladesh	5.39E-17	2.46E-17	5.32E-17
Belarus	0.00E+00	4.14E-18	6.90E-18
Belgium	4.21E-17	3.19E-17	3.51E-17
Belize	0.00E+00	0.00E+00	0.00E+00
Benin	0.00E+00	0.00E+00	0.00E+00
Bhutan	0.00E+00	0.00E+00	0.00E+00
Bolivia	3.99E-12	1.07E-13	1.54E-13
Bosnia and Herzegovina	7.73E-15	1.36E-14	3.93E-14
Botswana	4.57E-16	1.33E-15	1.02E-15
Brazil	5.54E-15	3.30E-15	7.27E-15
Brunei Darussalam	0.00E+00	0.00E+00	0.00E+00
Bulgaria	4.55E-15	9.14E-15	1.08E-14
Burkina Faso	0.00E+00	0.00E+00	6.09E-18
Burundi	0.00E+00	0.00E+00	0.00E+00
Cambodia	4.81E-16	1.63E-16	5.62E-16
Cameroon	2.98E-16	1.69E-16	1.69E-16
Canada	2.28E-16	3.77E-17	3.02E-17
Canarias	0.00E+00	0.00E+00	0.00E+00
Cayman Islands	0.00E+00	0.00E+00	0.00E+00
Central African Republic	0.00E+00	1.26E-16	9.69E-17
Chad	0.00E+00	0.00E+00	6.34E-18
Chile	6.66E-14	9.48E-15	2.94E-14
China	5.04E-16	6.75E-16	2.32E-15
Colombia	5.48E-12	3.25E-13	9.80E-14
Comoros	0.00E+00	0.00E+00	0.00E+00
Congo	1.91E-15	1.41E-15	1.54E-15
Congo DRC	2.86E-16	2.25E-16	3.03E-16
Cook Islands			
Costa Rica	5.42E-15	1.54E-14	2.79E-14
Côte d'Ivoire	1.54E-16	8.63E-17	5.52E-17
Croatia	7.80E-17	9.06E-17	1.41E-16
Cuba	4.14E-12	3.58E-13	2.76E-13
Cyprus	0.00E+00	0.00E+00	0.00E+00
Czech Republic	4.24E-17	1.73E-17	1.52E-17
Denmark	0.00E+00	9.77E-18	0.00E+00
Djibouti	0.00E+00	0.00E+00	0.00E+00
Dominican Republic	0.00E+00	0.00E+00	0.00E+00
Ecuador	6.66E-14	1.76E-14	7.44E-14
Egypt	1.05E-15	2.24E-15	4.07E-16
El Salvador	0.00E+00	0.00E+00	0.00E+00
Equatorial Guinea	0.00E+00	0.00E+00	0.00E+00
Eritrea	6.69E-16	4.44E-16	2.51E-16
Estonia	0.00E+00	0.00E+00	0.00E+00
Ethiopia	1.19E-15	9.14E-16	8.58E-16
Falkland Islands	0.00E+00	0.00E+00	0.00E+00
Fiji			
Finland	0.00E+00	0.00E+00	0.00E+00

France	5.04E-16	4.19E-16	4.92E-16
French Guiana	0.00E+00	0.00E+00	0.00E+00
French Polynesia			
French Southern Territories			
Gabon	5.53E-16	5.37E-16	6.25E-16
Gambia	2.17E-13	5.08E-14	3.16E-14
Georgia	2.49E-15	4.00E-15	3.03E-15
Germany	3.57E-16	2.30E-16	5.39E-16
Ghana	4.52E-17	3.71E-17	3.13E-17
Greece	2.25E-14	4.10E-14	5.58E-14
Greenland			
Guadeloupe	0.00E+00	0.00E+00	0.00E+00
Guatemala	2.75E-14	6.05E-15	1.15E-14
Guinea	1.64E-16	6.79E-17	6.04E-17
Guinea-Bissau	0.00E+00	0.00E+00	0.00E+00
Guyana	0.00E+00	9.02E-17	4.28E-16
Haiti	3.20E-13	1.54E-13	1.14E-13
Honduras	5.45E-15	4.16E-16	2.78E-16
Hungary	3.98E-17	2.17E-17	1.62E-17
Iceland	0.00E+00	0.00E+00	0.00E+00
India	6.55E-16	3.21E-16	1.50E-15
Indonesia	8.72E-16	1.03E-15	9.22E-16
Iran	9.17E-14	2.16E-14	1.92E-14
Iraq	3.47E-15	3.89E-15	7.63E-15
Ireland	0.00E+00	0.00E+00	1.08E-17
Israel	0.00E+00	0.00E+00	0.00E+00
Italy	1.44E-12	6.15E-13	1.31E-13
Jamaica	0.00E+00	0.00E+00	0.00E+00
Japan	1.74E-15	4.31E-16	1.41E-15
Jersey	0.00E+00	0.00E+00	0.00E+00
Jordan	1.76E-15	1.17E-15	1.21E-15
Kazakhstan	1.06E-14	8.85E-15	3.31E-14
Kenya	1.26E-16	1.56E-16	4.03E-16
Kiribati			
Kuwait	0.00E+00	0.00E+00	0.00E+00
Kyrgyzstan	1.41E-15	1.62E-15	1.98E-15
Laos	8.80E-16	3.83E-16	1.15E-15
Latvia	0.00E+00	0.00E+00	0.00E+00
Lebanon	0.00E+00	0.00E+00	0.00E+00
Lesotho	1.47E-15	4.18E-15	9.32E-15
Liberia	0.00E+00	0.00E+00	0.00E+00
Libya	1.21E-15	4.53E-16	2.59E-16
Lithuania	0.00E+00	0.00E+00	0.00E+00
Luxembourg	0.00E+00	0.00E+00	0.00E+00
Madagascar	1.00E-15	1.34E-15	4.75E-15
Madeira	0.00E+00	0.00E+00	0.00E+00
Malawi	0.00E+00	0.00E+00	0.00E+00
Malaysia	9.96E-16	6.05E-16	1.15E-15
Maldives			
Mali	0.00E+00	0.00E+00	4.86E-18
Mauritania	0.00E+00	0.00E+00	1.90E-17
Mauritius	0.00E+00	0.00E+00	0.00E+00
Mexico	7.02E-13	4.89E-14	7.46E-14
Moldova	1.57E-16	7.78E-17	1.18E-16
Mongolia	9.35E-18	1.24E-17	2.07E-17
Montenegro	0.00E+00	0.00E+00	0.00E+00
Morocco	1.58E-15	1.32E-15	3.83E-15
Mozambique	9.06E-15	1.68E-14	3.37E-14
Myanmar	2.16E-16	1.79E-16	4.40E-16
Namibia	6.72E-15	6.41E-15	1.28E-15
Nepal	1.99E-16	1.42E-16	8.49E-16
Netherlands	0.00E+00	2.12E-17	3.04E-17
New Caledonia			

New Zealand	0.00E+00	0.00E+00	0.00E+00
Nicaragua	2.07E-15	5.54E-16	3.92E-15
Niger	0.00E+00	0.00E+00	0.00E+00
Nigeria	9.61E-16	8.41E-16	2.26E-16
North Korea	1.44E-16	9.88E-17	2.13E-16
Norway	0.00E+00	0.00E+00	0.00E+00
Oman	1.01E-12	3.10E-13	1.57E-13
Pakistan	9.27E-15	5.46E-15	1.08E-14
Palestinian Territory	0.00E+00	0.00E+00	0.00E+00
Panama	0.00E+00	0.00E+00	0.00E+00
Papua New Guinea	0.00E+00	0.00E+00	0.00E+00
Paraguay	3.88E-16	4.66E-17	1.98E-16
Peru	8.40E-13	2.49E-14	1.31E-13
Philippines	9.77E-15	1.34E-14	2.85E-14
Poland	2.98E-17	1.45E-17	2.09E-17
Portugal	0.00E+00	0.00E+00	0.00E+00
Puerto Rico	0.00E+00	0.00E+00	0.00E+00
Qatar	0.00E+00	0.00E+00	0.00E+00
Réunion	0.00E+00	0.00E+00	0.00E+00
Romania	7.65E-17	3.40E-17	2.14E-17
Russian Federation	1.02E-15	1.32E-15	1.53E-15
Rwanda	4.20E-16	4.55E-16	2.50E-15
Saint Vincent and the Grenadines	0.00E+00	0.00E+00	0.00E+00
Samoa			
Saudi Arabia	1.02E-13	8.11E-14	1.03E-13
Senegal	3.53E-16	8.60E-16	1.43E-15
Serbia	5.69E-17	7.11E-17	1.41E-16
Sierra Leone	2.15E-16	1.04E-16	1.47E-16
Slovakia	3.67E-17	2.29E-17	3.58E-17
Slovenia	0.00E+00	0.00E+00	0.00E+00
Solomon Islands			
Somalia	0.00E+00	4.42E-17	3.66E-17
South Africa	3.39E-14	8.56E-14	2.40E-13
South Georgia			
South Korea	1.57E-17	7.37E-18	4.55E-17
South Sudan	0.00E+00	3.12E-17	3.67E-17
Spain	2.27E-15	5.23E-15	1.08E-14
Sri Lanka	1.40E-14	6.31E-15	2.70E-14
Sudan	5.80E-17	3.77E-17	7.07E-18
Suriname	7.18E-16	5.19E-16	1.26E-15
Swaziland	0.00E+00	0.00E+00	0.00E+00
Sweden	4.11E-17	1.34E-17	2.32E-17
Switzerland	0.00E+00	0.00E+00	0.00E+00
Syria	1.31E-13	9.38E-14	3.15E-14
Tajikistan	0.00E+00	0.00E+00	0.00E+00
Tanzania	6.03E-16	4.24E-16	4.65E-16
Thailand	2.95E-16	1.40E-16	4.63E-16
The Former Yugoslav Republic of Macedonia	0.00E+00	0.00E+00	0.00E+00
Timor-Leste	0.00E+00	0.00E+00	0.00E+00
Togo	0.00E+00	6.03E-17	4.91E-17
Trinidad and Tobago	0.00E+00	0.00E+00	0.00E+00
Tunisia	2.70E-15	1.67E-15	6.98E-16
Turkey	1.52E-14	1.68E-14	1.39E-14
Turkmenistan	1.45E-13	5.79E-14	6.18E-14
Turks and Caicos Islands			
Uganda	1.69E-15	1.27E-15	1.25E-15
Ukraine	3.78E-17	6.49E-17	3.74E-17
United Arab Emirates	4.53E-12	2.62E-12	4.83E-13
United Kingdom	6.89E-18	7.54E-18	1.59E-17
United States	6.76E-16	3.22E-16	3.03E-16
Uruguay	8.95E-16	1.96E-16	3.05E-16

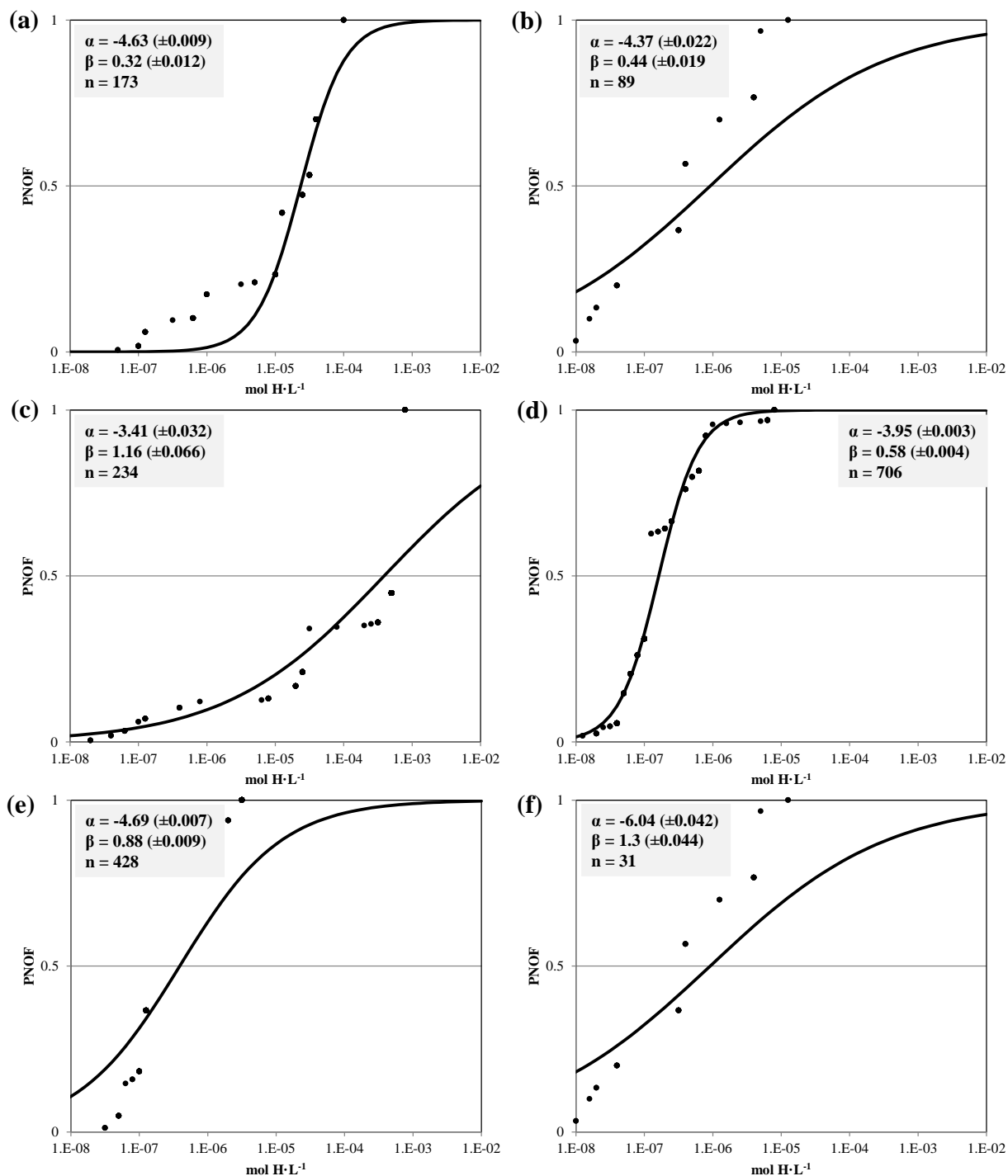| US Virgin Islands	0.00E+00	0.00E+00	0.00E+00
Uzbekistan	3.06E-13	1.33E-13	1.70E-13
Vanuatu			
Venezuela	3.26E-15	7.76E-16	4.68E-16
Vietnam	2.08E-16	9.75E-17	2.50E-16
Yemen	5.56E-15	7.64E-14	6.88E-14
Zambia	1.41E-16	7.49E-16	6.26E-16
Zimbabwe	1.18E-16	3.62E-16	6.02E-16

Table 7.2: Global endpoint characterization factors (PD·Fkg^{-1}·yr) on a continental level, based on vascular plant richness for SO$_2$, NO$_x$, and NH$_3$.

CONTINENT	CF SO$_2$ [PDF·yr/kg]	CF NOx [PDF·yr/kg]	CF NH$_3$ [PDF·yr/kg]
Asia	2.14E-14	2.69E-14	5.73E-15
North America	1.08E-13	7.75E-15	1.82E-14
Europe	2.40E-14	3.89E-14	1.21E-14
Africa	1.65E-14	2.02E-14	1.22E-14
South America	7.07E-13	2.83E-14	2.23E-14
Australia	4.60E-14	9.58E-14	1.32E-14

7.5. References

Azevedo, L. B. (2014). Development and application of stressor – response relationships of nutrients. Chapter 8. Ph.D. Dissertation, Radboud University Nijmegen, The Netherlands. http://repository.ubn.ru.nl.

Azevedo, L. B., van Zelm, R., Hendriks, A. J., Bobbink, R. and Huijbregts, M. A. J. (2013). "Global assessment of the effects of terrestrial acidification on plant species richness." Environmental Pollution **174**(0): 10-15.

Evans, M. and Jingqiu, M. (2009). "Updated Chemical Reactions Now Used in GEOS-Chem v8-02-01 Through GEOS-Chem v8-02-03." Oxidants and Chemistry Working Group Retrieved June 6th, 2011, from http://acmg.seas.harvard.edu/geos/wiki_docs/chemistry/chemistry_updates_v5.pdf.

Falkengren-Grerup, U. (1986). "Soil acidification and vegetation changes in deciduous forest in Southern-Sweeden." Oecologia **70**(3): 339-347.

IIASA. (2015). "ECLIPSE V5 global emission fields." Retrieved 10 September, 2016, from http://www.iiasa.ac.at/web/home/research/researchPrograms/air/ECLIPSEv5.html.

Jackson, R. B., Canadell, J., Ehleringer, J. R., Mooney, H. A., Sala, O. E. and Schulze, E. D. (1996). "A global analysis of root distributions for terrestrial biomes." Oecologia **108**(3): 389-411.

Kier, G., Kreft, H., Lee, T. M., Jetz, W., Ibisch, P. L., Nowicki, C., Mutke, J. and Barthlott, W. (2009). "A global assessment of endemism and species richness across island and mainland regions." PNAS **106**(23): 9322-9327.

NOAA. (2005). "National Climatic Data Center State of the Climate: Global Analysis for Annual 2005." Retrieved June 5th, 2011, from www.ncdc.noaa.gov/sotc/global/2005/13.

Olson, D. M., Dinerstein, E., Wikramanayake, E. D., Burgess, N. D., Powell, G. V. N., Underwood, E. C., D'Amico, J. A., Itoua, I., Strand, H. E., Morrison, J. C., Loucks, C. J., Allnutt, T. F., Ricketts, T. H., Kura, Y., Lamoreux, J. F., Wettengel, W. W., Hedao, P. and Kassem, K. R. (2001). "Terrestrial ecoregions of the worlds: A new map of life on Earth." Bioscience **51**(11): 933-938.

Roem, W. J. and Berendse, F. (2000). "Soil acidity and nutrient supply ratio as possible factors determining changes in plant species diversity in grassland and heathland communities." Biological Conservation **92**(2): 151-161.

Roy, P.-O., Azevedo, L. B., Margni, M., van Zelm, R., Deschênes, L. and Huijbregts, M. A. J. (2014). "Characterization factors for terrestrial acidification at the global scale: A systematic analysis of spatial variability and uncertainty." Science of The Total Environment **500–501**: 270-276.

Roy, P.-O., Deschênes, L. and Margni, M. (2012a). "Life cycle impact assessment of terrestrial acidification: Modeling spatially explicit soil sensitivity at the global scale." Environmental Science & Technology **45**(15): 8270–8278.

Roy, P.-O., Deschênes, L., Margni, M. and Huijbregts, M. A. J. (2012b). "Spatially-differentiated atmospheric source-receptor relationships for nitrogen oxides, sulfur oxides and ammonia emissions at the global scale for life cycle impact assessment." Atmospheric Environment **62**: 74-81.

van Zelm, R., Huijbregts, M. A. J., Van Jaarsveld, H. A., Reinds, G. J., De Zwart, D., Struijs, J. and Van de Meent, D. (2007). "Time horizon dependent characterization factors for acidification in life-cycle assessment based on forest plant species occurrence in Europe." Environmental Science & Technology **41**(3): 922-927.

Zvereva, E. L., Toivonen, E. and Kozlov, M. V. (2008). "Changes in species richness of vascular plants under the impact of air pollution: a global perspective." Global Ecology and Biogeography **17**(3): 305-319.

7.6.   Appendix

(a)
α = -4.63 (±0.009)
β = 0.32 (±0.012)
n = 173

(b)
α = -4.37 (±0.022)
β = 0.44 (±0.019
n = 89

(c)
α = -3.41 (±0.032)
β = 1.16 (±0.066)
n = 234

(d)
α = -3.95 (±0.003)
β = 0.58 (±0.004)
n = 706

(e)
α = -4.69 (±0.007)
β = 0.88 (±0.009)
n = 428

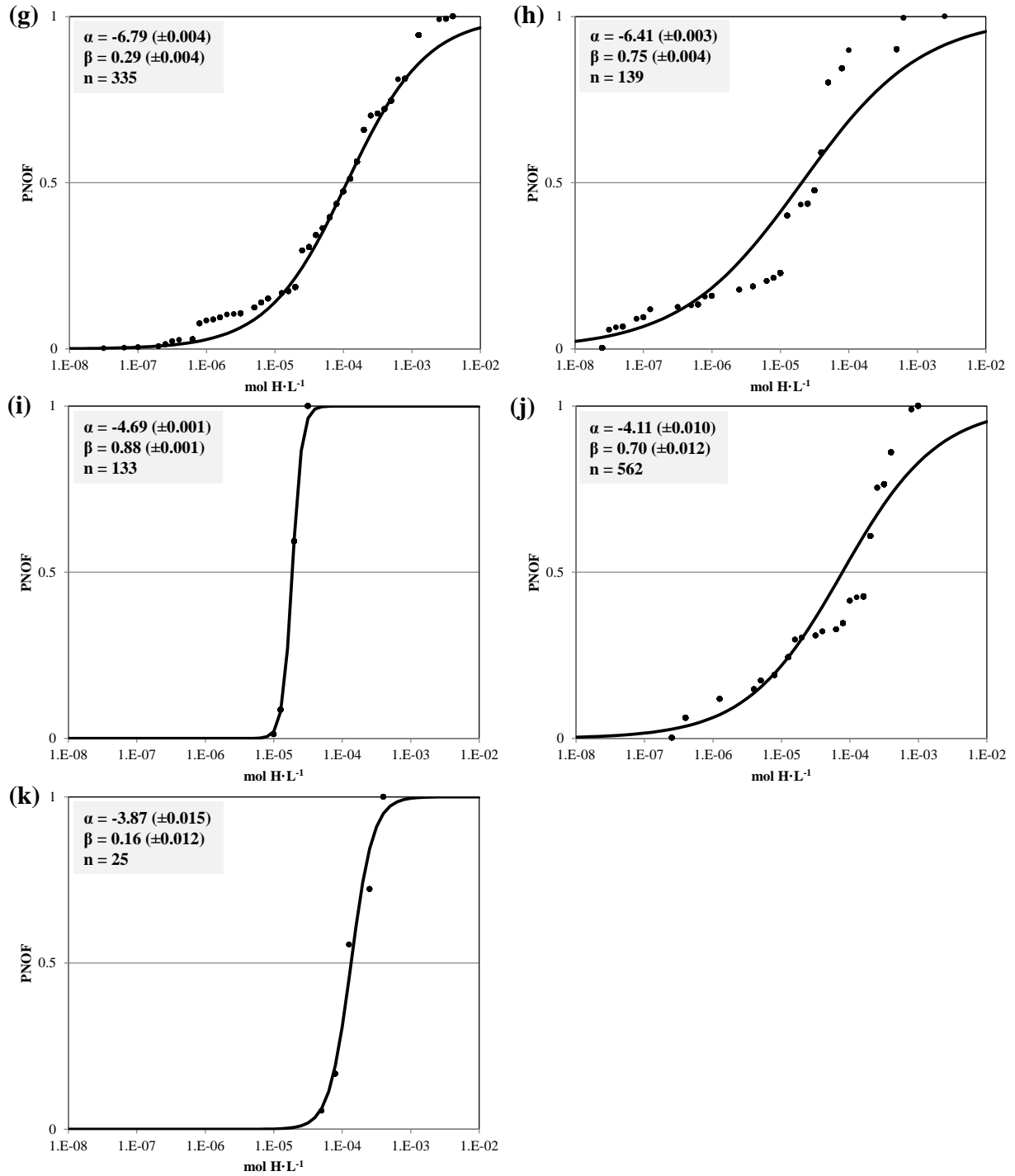**(f)**
α = -6.04 (±0.042)
β = 1.3 (±0.044)
n = 31

12

Figure 7.5: Coefficients α and β of the potentially not occurring fraction (PNOF) of vascular plant species as a logistic function of hydrogen ions (H, mol·L^{-1}) in the (a) tundra and alpine lands, (b) boreal forest and taiga, (c) temperate coniferous forest, and (d) temperate broadleaf mixed forest, (e) temperate grassland, savanna, and shrubland, (f) mediterranean forest, woodland, and scrub, (g) desert and xeric shrubland, (h) (sub)tropical dry broadleaf forest, (i) (sub)tropical grassland, savanna, and shrubland, (j) (sub)tropical moist broadleaf forest, and (k) mangrove.